16TH EUROPEAN CONFERENCE ON EARTHQUAKE ENGINEERING THESSALONIKI 18 - 21 JUNE 2018

PUSHOVER ANALYSIS FOR SEISMIC ASSESSMENT OF RC NIŠAVA BRIDGE

Mira PETRONIJEVIĆ[1], Miroslav MARJANOVIĆ[2], Dušan MILOJEVIĆ[3]

ABSTRACT

Contemporary structural design implies nonlinear behavior of ductile members for design seismic action. Therefore, the application of nonlinear analysis in the aseismic design of structures is required. Nonlinear static (pushover) analysis has become a very popular tool for the seismic assessment of structural performance during a particular earthquake due to the lower computational cost and less time consuming in comparison to the nonlinear time-history analysis. The standard pushover analysis (SPA) has been extended to the modal pushover analysis (MPA) of buildings in order to consider higher modes effects. Since the higher modes usually play an important role in the seismic bridge analysis, the MPA has been adopted for the seismic assessment of bridges.
In the paper, the MPA of the Nišava Bridge structure (233.2m long 7-span continuous bridge, curved in plan with R=540m and prestressed 13.75m wide bridge deck) has been performed in transverse direction, for two levels of excitation which are 2 and 3 times higher than the design level (a_g=0.1g). For the horizontal component of the seismic action, elastic response spectrum, Type 2 for soil type B, according to EN1998-1 has been selected. Analyses considering different levels of excitation and different monitoring points are carried out using the SAP2000 commercial software package.
The seismic demands of the structure (peak displacements of the deck in transverse direction), subjected to the monotonically increasing lateral forces have been calculated, considering five dominant transverse modes. Hinge distribution within the structure has been determined, too, for the target displacement obtained from the MPA. The overall performance of the bridge was very satisfactory. Neither local nor global failure was predicted, even under seismic actions that three times exceed the design level. The performed analysis showed that the fundamental transverse mode shape contributes to the final response significantly. The influence of higher modes is more pronounced for higher level of excitation.

Keywords: modal pushover analysis, capacity spectrum method, multi-span curved bridge

1. INTRODUCTION

In recent years, increasing attention has been paid to the analysis of the earthquake impact on bridges. The reason for this is the collapse of bridges that have occurred in areas with high seismicity. EU has adopted standard EN 1998-2 (2006) that recognized the need for reliable estimation of the nonlinear seismic response of bridges. Standard prescribes two nonlinear methods for the analysis and design of earthquake resistant bridges: (a) the nonlinear response-history analysis (NRHA) and (b) the nonlinear static pushover analysis.
NRHA gives the best insight into the dynamic response of the structure, but it is a complex and time-consuming for everyday engineering practice. Therefore, the simplified nonlinear static pushover analysis is increasingly used for seismic design and assessment of bridges. There are several nonlinear pushover methods, mostly developed for the analysis of buildings, which are further extended for the analysis of bridges: standard pushover analysis (SPA), multi-modal pushover analysis (MPA), multi-modal adaptive pushover (MAP).
SPA, which is also known as the single-mode non-adaptive method, is the simplest method based on

[1]Professor, University of Belgrade, Faculty of Civil Engineering, Belgrade, Serbia, pmira@grf.bg.ac.rs
[2]Assistant Professor, University of Belgrade, Faculty of Civil Engineering, mmarjanovic@grf.bg.ac.rs
[3]MSc Student, University of Belgrade, Faculty of Civil Engineering, dusan230293@gmail.com

the assumption that the response of the structure is governed by one predominant mode which remains constant during the seismic load changes. It is included into EN1998-2 in the form of the N2 method developed by Fajfar (Fajfar et al. 1997). MPA, developed by Chopra and Goel (2002) takes into account the influence of the higher modes, but still assumes that these modes remains constant and independent of the seismic intensity. It is also called multimode non-adaptive pushover method.

The more complex methods, called multi-modal adaptive pushover, take into account the influence of the higher modes as well as their changes based on the seismic intensity. These methods could be of the force-based or the displacement-based type (Pinho et al. 2007).

The detailed investigations of the effectiveness of such pushover schemes in assessing bridges subjected to seismic action are presented in the works of: (Pinho et al. 2007), Isaković and Fischinger (2006), (Isaković et al. 2008), Isaković and Fischinger (2014), (Paraskeva et al. 2006) and Paraskeva and Kappos (2010). The main conclusion of these investigations is that SPA methods are accurate enough for regular bridge configurations where the effective modal mass of the fundamental mode is at least 80% of the total mass (Isaković et al. 2008), (Paraskeva et al. 2006). When irregular bridges are considered, the advantages of using some of the MAP become evident (Pinho et al. 2007).

In the paper, results of the multi-modal pushover analysis of the Nišava Bridge (in transverse direction) are presented and discussed. Two different seismic intensities, as well as the two different monitoring points for estimating the displacement demand, were taken into account. The influence of higher modes is discussed. The hinge distribution within the structure is calculated for the target displacement obtained from the MPA.

2. DESCRIPTION OF STUDIED BRIDGE STRUCTURE

The Nišava Bridge was selected as the reference case for this analysis. It is a seven-span continuous bridge structure of 232.2m total length, illustrated in Figure 1. The bridge is curved-in-plan, with the radius of curvature R=540m and longitudinal slope of 1.82%.

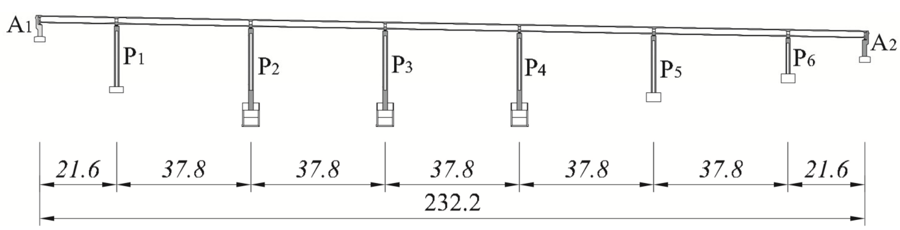

Figure 1. Structure layout in longitudinal direction

The deck is supported by six RC piers S_1-S_6 of unequal clear heights: P_1=17.14m, P_2=17.51m, P_3=16.82m, P_4=16.11m, P_5=16.07m and P_6=9.95m. All piers have rectangular hollow cross section (Figure 2a), resting on prismatic footings, firmly bonded to the surrounding rock. At bridge ends the RC abutments A_1 and A_2 are located.

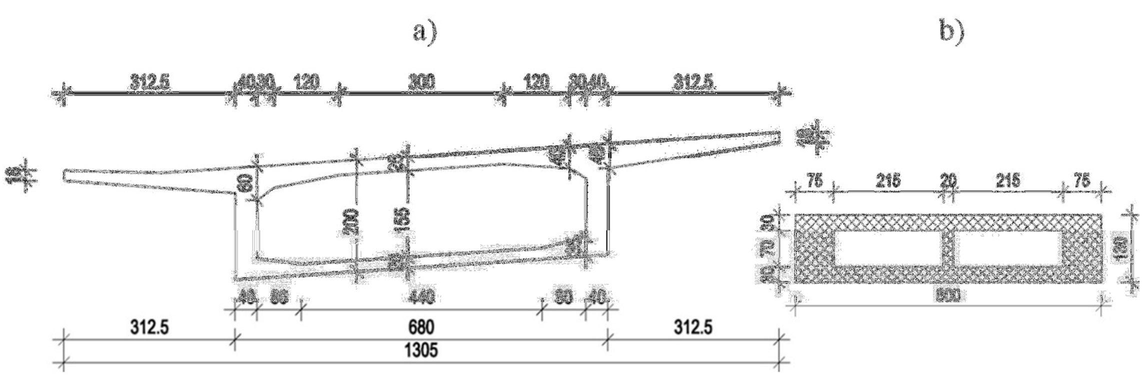

Figure 2. a) Cross section of the deck, b) cross section of the pier

The RC concrete deck consists of a prestressed box girder, 13.05m wide and 200cm high, with transverse inclination of 6.5% (Figure 2b). In the longitudinal direction, the deck webs thickness vary from 40-70cm, while the bottom plate thickness vary from 20-40cm. The deck is resting on piers over different type of "Neotopf" bearings. The inner piers (P_2-P_5) are monolithically connected to the deck, while for the outer piers (P_1 and P_6) a bearing type connection is adopted allowing movement in the tangential direction, but restricting the movement in radial direction. The rotation about both longitudinal and transverse axis was unrestrained in all connections.
The bridge has been designed according to Serbian regulations (1980) as an object of category I (objects of high importance), for VII seismic zone (PGA of 0.1g), and soil type I (equivalent to the soil type B of EN1998-1 (2006)). The adopted damping in transverse direction is ξ=7%. The reinforcement detailing according to Serbian regulations leads to the high amount of confinement of the joints, thus the structure is designed as a ductile structure allowing plastic hinge formation at the end of the piers.

3. NUMERICAL MODEL

The considered structure is modeled in SAP2000, Computers and Structures, Inc. (1998) using 3D beam elements. The material properties of RC members and steel reinforcement are given in Table 1.

Table 1. Material properties of RC members

Element	Material	E [GPa]	ν	γ[kN/m^3]	f_c' [MPa]	f_y [MPa]	f_u [MPa]
Column	C30/37	31.5	0.2	25.0	23.00	-	-
Pier	C35/45	35.0	0.2	25.0	27.75	-	-
Rebars	RA 400/500	210	0.3	78.5	-	400	500

An idealized deck cross section was adopted in the numerical model (Figure 3), neglecting the inclinations in longitudinal and lateral directions, as well as changes in geometry along the length.

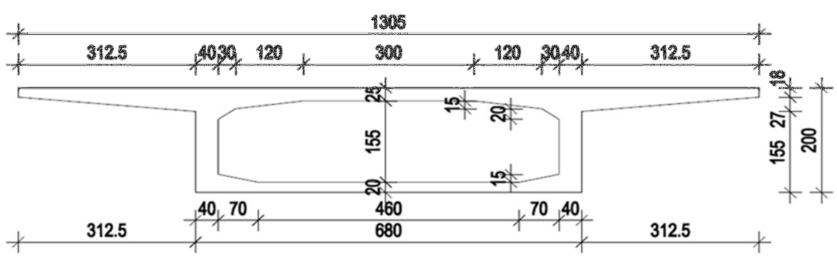

Figure 3. Simplified cross section of the bridge deck

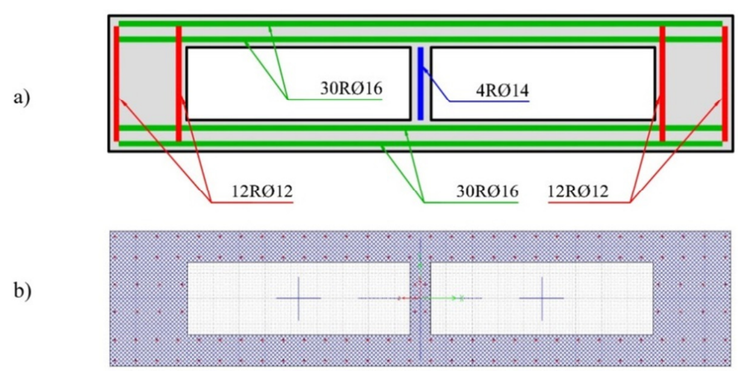

Figure 4. Reinforcement in piers: a) longitudinal bars, b) SAP2000 Section Designer cross section

The deck is supposed to remain in the elastic range. The torsional rigidity of the deck is reduced to 50% of the homogeneous cross section.

The reinforcement of the piers was adopted according to Ličina and Kovrlija (2010) and assigned using the Section Designer tool of SAP2000, Figure 4. Bending rigidity of the piers is reduced to 50%. Since the foundation soil is of the high capacity, the piers have been modeled as beams completely clamped at the bottom. The effect of soil-structure-interaction is neglected. The abutments are modeled using nonlinear springs (K_z = 1800000kN/m, K_{long} = 4644kN/m) and appropriate gap elements (K_{gap} = 1000kN/m, d_{gap} = 5cm).
Mass of the structure is generated from the self-weight, additional dead loadings and traffic loading, according to EN 1998-2. The weights of the structural elements are extracted from the Main Design of Nišava Bridge, Ličina and Kovrlija (2010). The self-weight of the model (generated automatically using the options of the SAP2000) is Q_G = 51441.2kN. The additional dead loading is $Q_{\Delta G}$ = 11038.8kN. The traffic loading is accounted as the 20% of the maximum traffic loading according to EN1998-2, and its total amount is Q_T = 2104.6kN. Therefore, the total weight of the structure for the seismic calculation is $Q = Q_G + Q_{\Delta G} + Q_S$ = 64584.6kN. Finally, the model has been discretized using 167 3D prismatic beam elements, having the approximate length of 2.3m.

4. MULTIMODAL PUSHOVER ANALYSIS

The bridge was assessed using the multimodal pushover analysis (MPA) in transverse direction. Two different levels of excitation were considered (a_g/g = 0.20 and a_g/g = 0.30), as well as two different monitoring points. For the horizontal component of the seismic action, elastic response spectrum $S_e(T)$, Type 2 for soil type B, according to EN1998-1 (2006) was used, with following parameters corresponding to the spectrum: S=1.00 T_B=0.05s, T_C=0.25s and T_D=1.20s.
Two selected monitoring points are: (i) the mass center of the bridge deck (MP1), and (ii) the resultant of the modal load pattern of the first transverse mode (3rd mode) (MP2), which location was calculates according to:

$$x^* = \frac{\sum_{j=1}^{N} x_j m_j \phi_{jn}}{\sum_{j=1}^{N} m_j \phi_{jn}} \tag{1}$$

where, x_j is the distance of the jth mass m_j from a (selected) point of the MDOF system and ϕ_{jn} is the value of ϕ_n at the jth mass m_j (Paraskeva et al. 2006). Locations of these two monitoring points are shown in Figure 5.

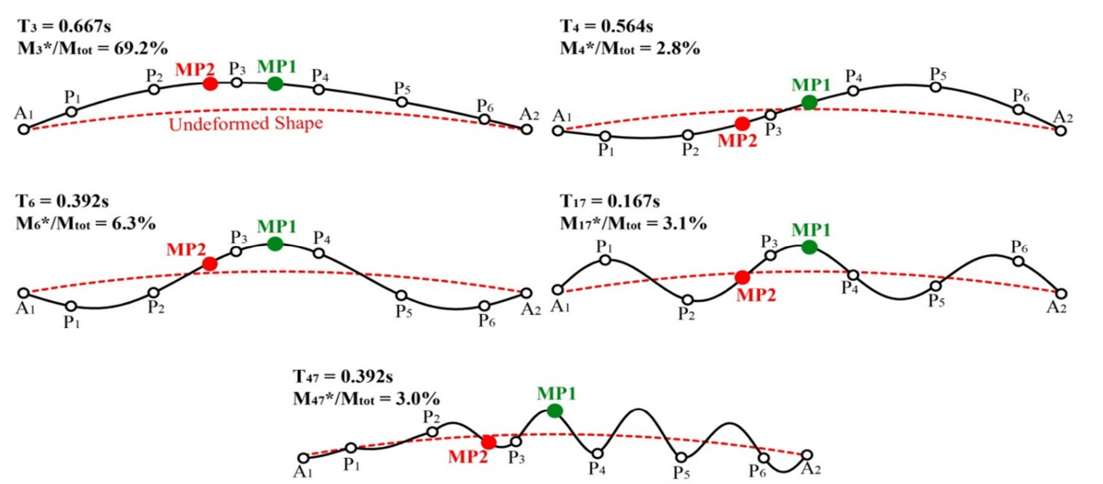

Figure 5. Transverse mode shapes, corresponding periods, effective modal masses, monitoring points MP1 and MP2 and pier locations P_i

The required dynamic properties (periods T_n and modes ϕ_n) were determined using standard eigenvalue analysis in SAP2000. Note that the obtained elastic periods correspond to the effective properties of the structure. In the MPA, only transverse modes which modal mass participation factors are higher than 1% are considered. The lowest obtained mode was the longitudinal one (T_1 = 2.56s), while the most dominant five transverse modes are 3rd, 4th, 6th, 17th and 47th. All other transverse modes have the modal mass participation factors less than 1%, so they were not taken into account. By taking these five transverse modes the 84.4% of the total mass in the transverse direction is considered. Since the common used rule of considering all modes whose masses captured 90% of the total mass of the structure has shown to be very rigid (Paraskeva et al. 2006), more than 80% of the total mass is considered acceptable. The obtained mode shapes with the corresponding periods and effective modal masses are shown in Figure 5.

It should be noted that slight non-symmetry of mode shapes originates from the different height of columns, thus the stiffness of the substructure is not equally distributed along the bridge.

The multi-mode pushover analysis (MPA) is proposed by Chopra and Goel (2002) in order to take into account higher modes of vibrations. According to Chopra and Goel (2002), the pushover analyses are carried out separately for each significant mode, and the contributions from individual modes to the calculated response quantities (displacements, drifts, etc.) are combined using an appropriate combination rule (SRSS or CQC).

In the pushover analysis the superstructure was modeled to remain elastic. The only inelastic behavior is allowed in the piers, according to EN 1998-2. The inelastic behavior in the piers was modeled using the software built-in P-M2-M3 plastic hinges, according to FEMA 356 (2000).

The elastic modal forces $s_n^*=\mathbf{m}\phi_n$ are applied as invariant seismic load patterns (where **m** is the mass matrix of the structure). Obtained modal pushover curves (V_{bn} - u_{rn}) for each mode (base shear vs. displacement of the monitoring point) are bilinearized using FEMA440 Displacement Modification procedure (2005) implemented in SAP2000. These curves are then converted to spectral acceleration, S_a, and spectral displacement, S_d, of an equivalent SDOF system, using modal conversion parameters:

$$S_a = \frac{V_{bn}}{M_n^*}, \qquad S_d = \frac{u_{rn}}{\Gamma_n \phi_{rn}} \tag{2}$$

where ϕ_{rn} is the value of the mode shape ϕ_n at the monitoring (reference) point, $M_n^* = L_n \Gamma_n$ is the effective modal mass, $L_n = \phi_n^T \mathbf{m} 1$, $\Gamma_n = L_n / M_n$ is the modal participation factor , and $M_n = \phi_n^T \mathbf{m} \phi_n$ is the generalized mass for the n^{th} mode. Note that gravity loads (self-weight + additional dead load + 20% of the live load according to EN1998-2) are applied before each pushover analysis, and P-Δ effects are included. The obtained capacity diagrams for an equivalent SDOF system are shown in Figure 6, along with the horizontal elastic response spectra for a_g/g = 0.20 and a_g/g = 0.30 in ADRS format.

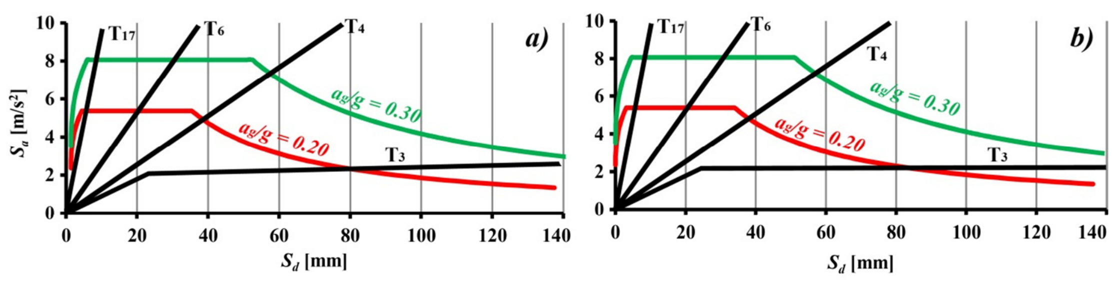

Figure 6 – Capacity curves for: a) the deck mass center, MP1, b) the resultant of modal forces for the first transverse mode, MP2. Elastic response spectra of en equivalent SDOF systems for both a_g/g = 0.20 (red line) and a_g/g = 0.30 (green line)

Obviously, the capacity curves corresponding to higher transverse modes (4, 6, 17 and 47) are linear which leads to the conclusion that the bridge does not reach the inelastic range when subjected to higher modes. Figure 5 shows that position of monitoring point MP1 provides the appropriate load pattern of the 3rd - 5th transverse modes, but not for the second transverse mode. Its effect on the response is relatively low due to the low effective mass participation factor (2.8%). Based on this can be concluded that i) the piers closest to the monitoring point do not enter the inelastic range in higher modes, and ii) despite the participation factor of the first transverse mode is less than 80% (69.2%), this mode is significant for the inelastic assessment of bridge. Therefore, μ = 1 for higher modes (n = 4, 6, 17 and 47), leading to the fact that $S_{a,in} = S_{ae}$, while the inelastic displacement demands $S_{d,rn}$ are equal to elastic displacement demands $S_{de,rn}$.

Table 2. Values of inelastic displacement demands $S_{d,rn}$ [mm] considering different monitoring points and different levels of earthquake excitation

a_g/g	mass center (MP1)				resultant of modal forces (MP2)			
	n=4	n=6	n=17	n=47	n=4	n=6	n=17	n=47
0.20	38.11	20.70	3.48	0.32	38.11	20.70	5.44	1.11
0.30	57.16	31.05	5.23	0.49	57.16	31.05	8.17	1.66

According to Figure 6, the structure exhibits the inelastic behavior only in the first transverse mode (mode 3). For inelastic behavior, the procedure for estimating the displacement demand at the monitoring point is based on the use of inelastic spectra. The inelastic spectra have been derived from the elastic spectra using the well-known relations:

$$S_{a,in} = \frac{S_{ae}}{R_\mu}, \qquad S_{d,in} = \frac{\mu}{R_\mu} S_{de} = \mu \left(\frac{T}{2\pi} \right)^2 S_{ae} \tag{3}$$

where $S_{a,in}$ and $S_{d,in}$ are inelastic spectral acceleration and spectral displacement, respectively, R_μ is the reduction factor:

$$R_\mu = \begin{cases} \mu & T \geq T_C \\ (\mu - 1)\dfrac{T}{T_C} + 1 & T < T_C \end{cases} \tag{4}$$

while μ is ductility demand. The ductility demands, which are easily extracted from the known capacity curve and elastic spectra in the ADRS format $(\mu = S_{de,u} / S_{de,y})$, are given in Table 3.

Inelastic spectra for both considered levels of excitation have been obtained according to Eq. (3), and shown in Figure 7 together with two capacity curves obtained for the first transverse mode (n=3) at two different monitoring points. Note that the elastic branch of the capacity curves for MP1 and MP2 in Figure 7 is the same, because it is related to the elastic properties of the bridge, only small differences occur in the inelastic range. Inelastic displacement demands $S_{d,r3}$ are extracted from Figure 7 and are given in Table 4.

Inelastic response quantities of the actual bridge are separately obtained for each individual mode from the inelastic SDOF system and convert to the MDOF system. The conversion from the equivalent SDOF to the MDOF system is performed using the following equation, for the nth mode:

$$u_{r,n} = S_{d,rn} \Gamma_n \phi_n \tag{5}$$

where $u_{r,n}$ is the modal displacement demand along the actual bridge deck, while $S_{d,rn}$ is the inelastic modal displacement demand of the SDOF (at the location of the monitoring point) obtained from the inelastic spectrum.

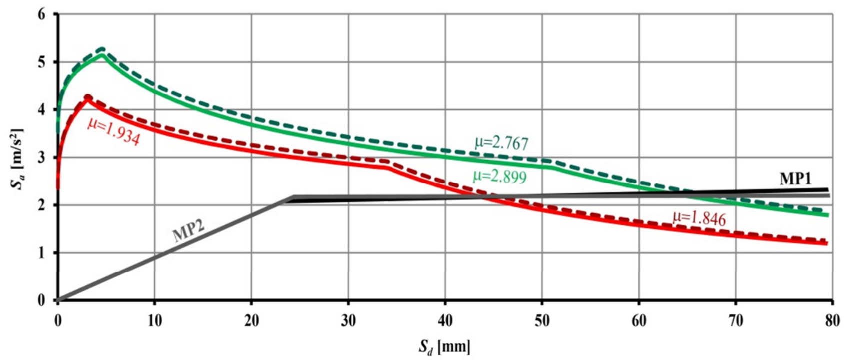

Figure 7. Inelastic spectra of the first transverse mode (n=3) for a_g/g = 0.20 (red lines) and a_g/g = 0.30 (green lines), considering different ductility demands and capacity curves of two different monitoring points: MP1 – black line, MP2 – grey

Table 3. Ductility demands μ for the first transverse mode (n=3) for different monitoring points and different levels of earthquake excitation

Monitoring point	$\mathbf{a_g/g = 0.20}$	$\mathbf{a_g/g = 0.30}$
mass center (MP1)	1.934	2.899
modal force resultant (MP2)	1.846	2.767

Table 4. Inelastic displacement demands $S_{d,r3}$ [mm] considering different monitoring points and different levels of earthquake excitation

Monitoring point	$\mathbf{a_g/g = 0.20}$	$\mathbf{a_g/g = 0.30}$
mass center (MP1)	42.19	61.25
modal force resultant (MP2)	43.55	65.33

The SRSS estimation of the total response $u_{r,SRSS}$ of the bridge is calculated from the following equation:

$$u_{r,SRSS} = \sqrt{\sum_{n=1}^{N} u_{r,n}^2} \tag{6}$$

Figures 8-11 illustrate the transverse deck displacements along the bridge for 5 significant modal patterns in the transverse direction, as well as the total deck displacements obtained by applying the SRSS combination rule.

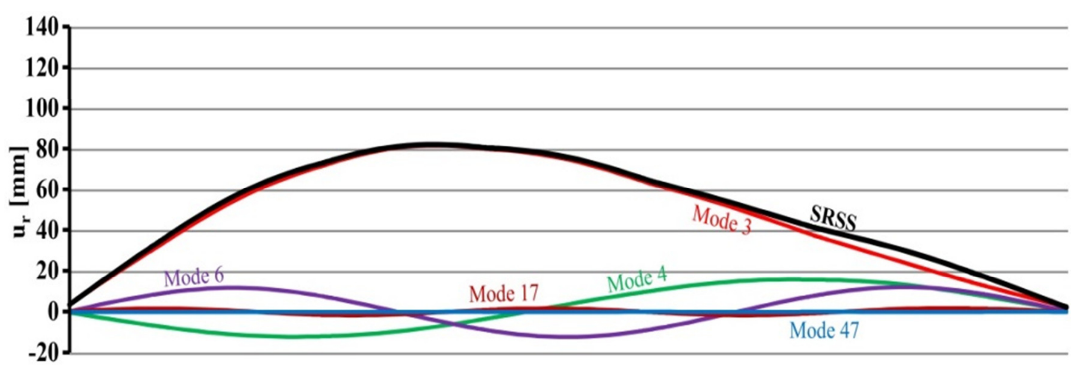

Figure 8 – Deck displacements due to the horizontal elastic response spectrum, a_g/g=0.20 calculated using monitoring point MP1

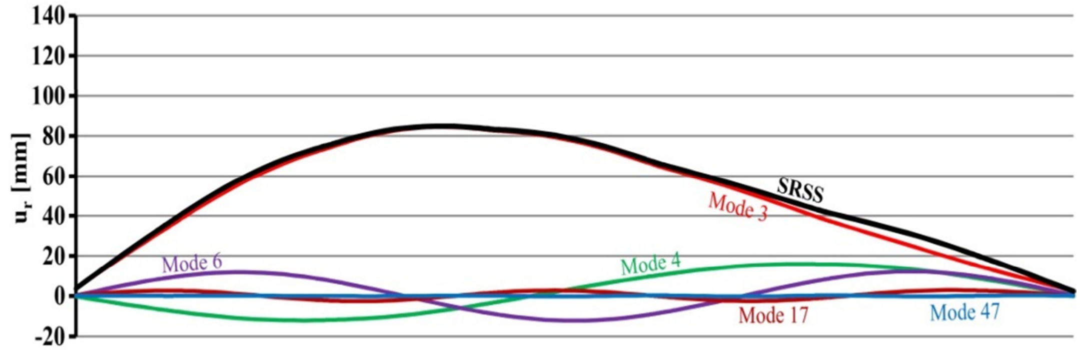

Figure 9 – Deck displacements due to the horizontal elastic response spectrum, a_g/g=0.20 calculated using monitoring point MP2

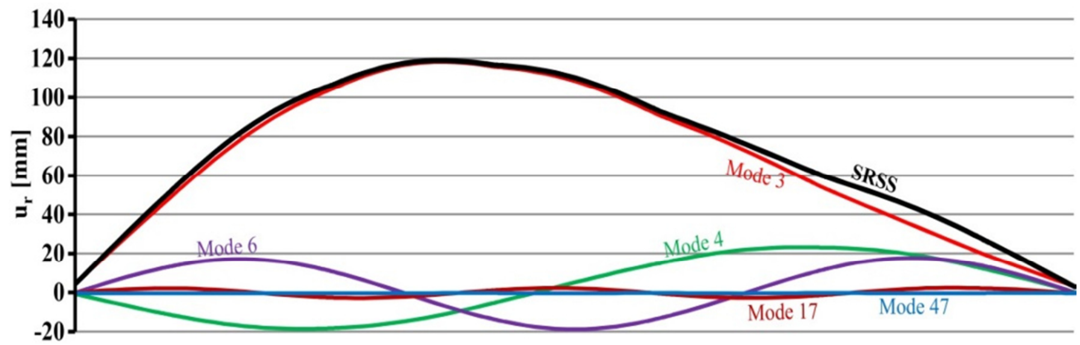

Figure 10 – Deck displacements due to the horizontal elastic response spectrum, a_g/g=0.30 calculated using monitoring point MP1

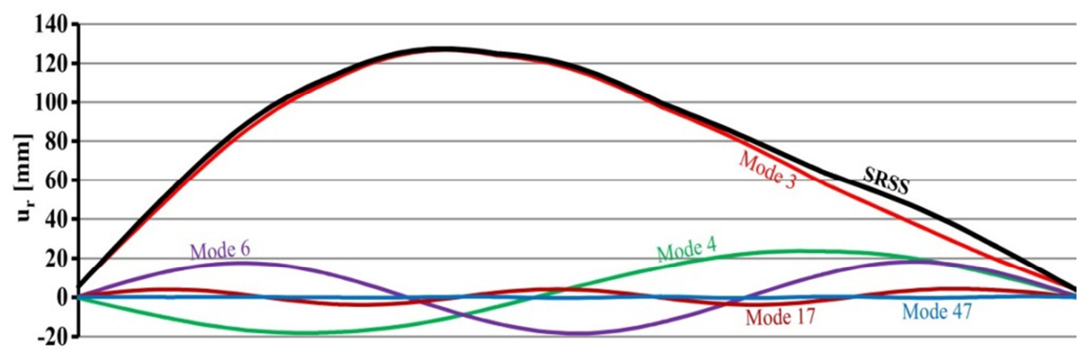

Figure 11 – Deck displacements due to the horizontal elastic response spectrum, a_g/g=0.30 calculated using monitoring point MP2

Figures 8-11 confirm former statement that the first transverse mode (mode 3) contributes to the final response significantly. The influence of higher modes is more pronounced for higher level of excitation (a_g/g=0.30), especially towards the right-hand side of the bridge.

Figure 12 shows the comparison between peak modal responses obtained for all investigated cases. For both considered levels of excitation, it is obvious that higher peak modal displacements have been obtained for the monitoring point MP2 at the location of the resultant of modal forces, in comparison with the monitoring point MP1 at the location of mass center of the bridge deck. The differences are 3.2% for a_g/g=0.20, and 6.6% for a_g/g=0.30.

For the determination of plastic hinge distribution within the structure, the bridge structure is finally pushed to the value of peak displacement. The modal force distribution considers the first transverse mode (mode 3), which proved to be dominant in transverse direction. The formation of plastic hinges is shown in Figure 13.

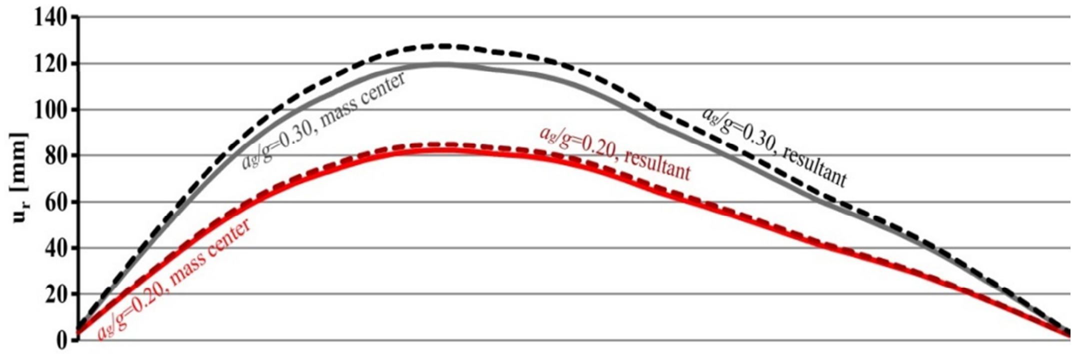

Figure 12 – Bridge response to the horizontal elastic response spectrum according to EN1998-1, considering different a_g/g ratios and different monitoring points

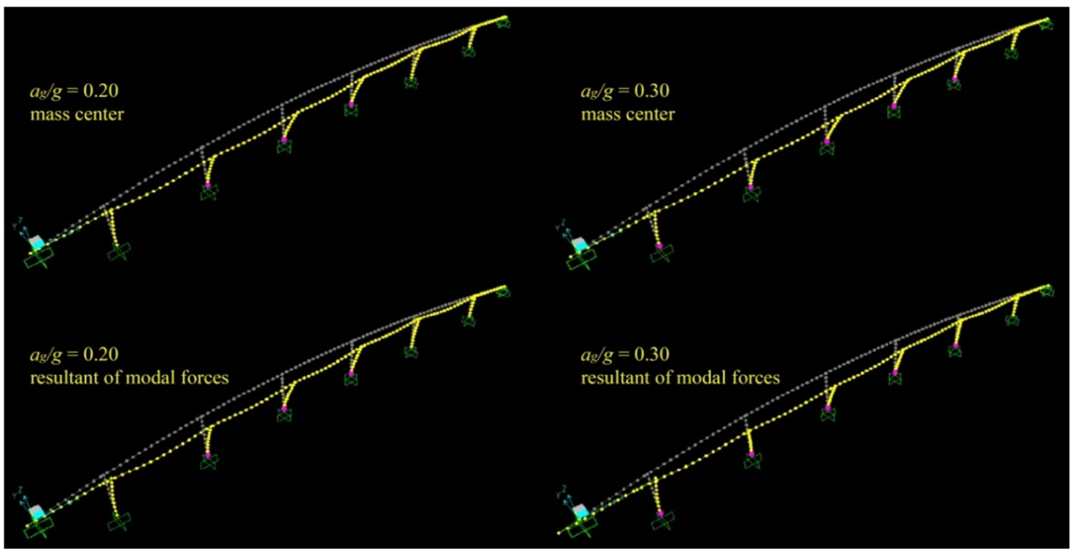

Figure 13. Plastic hinges formation for two different monitoring points and two levels of excitation

Obviously, for a_g/g=0.20, the plastic hinges have been formed in piers P2-P4, while for a_g/g=0.30, the hinges have been formed in piers P1-P5. The level of hinge formation is **B** according to FEMA 356, thus the bending moment in piers reached the yield limit.

5. CONCLUSIONS

In the paper, the multimodal pushover analysis (MPA) of the Nišava Bridge structure has been performed in transverse direction, for two levels of excitation which are 2 and 3 times higher than the design level ($a_g=0.1g$). For the horizontal component of the seismic action, elastic response spectrum, $S_e(T)$, Type 2 for soil type B, according to EN1998-1 has been selected.

The seismic demands of the structure (peak displacements of the deck in transverse direction), subjected to the monotonically increasing lateral forces have been calculated, considering five transverse modes which modal mass participation ratio is higher than 1%. The hinge distribution within the structure has been calculated, too, for the target displacement obtained from the MPA.

The overall performance of the bridge was very satisfactory. Neither local nor global failure was predicted, even under seismic actions that three times exceed the design level. A significant overstrength of the bridge was found due to the partial safety factors used in the design, minimum reinforcement due to the Serbian code requirements, and application of code provisions related to the longitudinal bar buckling (high amount of confinement of joints).

The performed analysis showed that the fundamental transverse mode shape contributes to the final response significantly, although its modal participation factor is less than 80%. The influence of higher modes is more pronounced for higher level of excitation (a_g/g=0.30), especially towards the right-hand side of the bridge. For both considered levels of excitation, higher peak modal displacements have been obtained for the monitoring point at the location of the resultant of modal forces (MP2), in comparison with the monitoring point at the location of mass center (MP1) of the bridge deck. For a_g/g=0.20, the bending moment reached the yield point in piers P_2-P_4, while for a_g/g=0.30, the yield point has been reached in P_1-P_5.

6. ACKNOWLEDGMENTS

The financial support of the Ministry of Education, Science and Technological Development, Republic of Serbia, through the projects TR-36043 and TR-36048, is acknowledged. The authors express their gratitude to Zoran Kovrlija, MSc. CE and Željko Ličina, MSc. CE (designers of the bridge structure) for providing the technical details of the structure.

7. REFERENCES

Chopra AK, Goel RK (2002). A modal pushover analysis procedure for estimating seismic demands for buildings. *Earthquake Engineering and Structural Dynamics*, 31(3): 561–582.

Computers and Structures, Inc. (1998). SAP2000: Integrated Finite Element Analysis and Design of Structures. Berkeley, California, USA.

European Committee for Standardisation (2006). Eurocode 8 - Design of structures for earthquake resistance - Part 1: General rules, seismic actions and rules for buildings. Brussels, Belgium.

European Committee for Standardisation (2006). Eurocode 8 - Design of structures for earthquake resistance - Part 2: Bridges. Brussels, Belgium.

Fajfar P, Gašperšič P, Drobnič D (1997). A simplified nonlinear method for seismic damage analysis of structures. *Proceedings of the International Workshop: Seismic Design Methodologies for the Next Generation of Codes,* Bled, Slovenia, 183–194.

Federal Emergency Management Agency (2000). *FEMA 356: Prestandard and commentary for the Seismic Rehabilitation of Buildings*. Washington, DC, USA.

Federal Emergency Management Agency (2005). *FEMA 440: Improvement of nonlinear static seismic analysis procedures*. Washington, DC, USA.

Isaković T, Fischinger M (2006). Higher modes in simplified inelastic seismic analysis of single column bent viaducts. *Earthquake Engineering and Structural Dynamics,* 35: 95–114.

Isaković T, Fischinger M (2014). Seismic Analysis and Design of Bridges with an Emphasis to Eurocode Standards. In: Ansal A (ed) Perspectives on European Earthquake Engineering and Seismology, *Geotechnical, Geological and Earthquake Engineering* 34, Springer Netherlands, pp. 195-225.

Isaković T, Lazaro MPN, Fischinger M (2008). Applicability of pushover methods for the seismic analysis of single-column bent viaducts. *Earthquake Engineering and Structural Dynamics*, 37: 1185–1202.

Ličina Ž, Kovrlija Z (2010). Main Design of Nišava Bridge (in Serbian). Institute of Transportation CIP, Belgrade, Serbia.

Pinho R, Casatotti C, Antoniou S (2007). A comparison of single-run pushover analysis techniques for seismic assessment of bridges. *Earthquake Engineering and Structural Dynamics,* 36: 1347–1326.

Paraskeva TS, Kappos AJ, Sextos AG (2006). Extension of modal pushover analysis to seismic assessment of bridges. *Earthquake Engineering and Structural Dynamics*, 35: 1269–1293.

Paraskeva TS, Kappos AJ (2010). Further development of a multimodal pushover analysis procedure for seismic assessment of bridges. *Earthquake Engineering and Structural Dynamics,* 39: 211-222.

Regulations of Technical Normative for the construction of high building objects in seismic areas (1980).